JOURNAL OF PHYSIOLOGY AND PHARMACOLOGY 2020, 71, 3, 437-450
www.jpp.krakow.pl | DOI: 10.26402/jpp.2020.3.15

L. KU[1], J. LEE[1], J.W. LIM[1], L. JIN[2], J.T. SEO[2], H. KIM[1]

DOCOSAHEXAENOIC ACID INHIBITS ETHANOL/PALMITOLEIC ACID-INDUCED NECROPTOSIS IN AR42J CELLS

[1]Department of Food and Nutrition, College of Human Ecology, Yonsei University, Seoul, Republic of Korea;
[2]Department of Oral Biology, Yonsei University College of Dentistry, Seoul, Republic of Korea

Fatty acid ethyl esters (FAEEs), non-oxidative metabolites of ethanol, are the main causative agents of severe acute pancreatitis resulting from alcohol abuse. Pancreatic acinar cells exposed to ethanol in combination with the fatty acid palmitoleic acid (EtOH/POA) display increased levels of palmitoleic acid ethyl ester and cell death. Oxidative stress and acinar cell necroptosis are implicated in the pathology of severe acute pancreatitis. Docosahexaenoic acid (DHA) serves as a powerful anti-oxidant that reduces pancreatic inflammation and improves the outcomes of patients with acute pancreatitis. We investigated whether treatment of EtOH/POA, as an *in vitro* model of alcoholic pancreatitis, increases reactive oxygen species (ROS), necroptosis-regulating proteins, and cell death by increasing nicotinamide adenine dinucleotide phosphate (NADPH) oxidase activity and intracellular calcium. Also, we investigated whether DHA inhibits EtOH/POA-induced alterations in pancreatic acinar AR42J cells. As a result, EtOH/POA increased intracellular and mitochondrial ROS levels, NADPH oxidase activity, necroptosis-regulating proteins, and cell death, which was inhibited by NADPH oxidase inhibitor apocynin, the Ca^{2+} chelator BAPTA, and DHA. However, DHA did not reduce EtOH/POA-induced increases in Ca^{2+} oscillation or levels in AR42J cells. Furthermore, EtOH/POA induced mitochondrial dysfunction by reducing mitochondrial membrane polarization and hence, adenosine triphosphate (ATP) production. DHA treatment attenuated EtOH/POA-induced mitochondrial dysfunction. In conclusion, DHA inhibits EtOH/POA-induced necroptosis by suppressing NADPH oxidase activity, reducing ROS levels, preventing mitochondrial dysfunction, and inhibiting activation of necroptosis-regulating proteins in AR42J cells.

Key words: *docosahexaenoic acid, ethanol, necroptosis, fatty acid ethyl esters, palmitoleic acid, pancreatitis, reactive oxygen species, mitochondrial dysfunction*

INTRODUCTION

Acute pancreatitis (AP) is a sudden onset, necro-inflammatory disease of the exocrine pancreas. Although conservative management usually results in clinical improvement for most patients with AP, 20% of all cases develop extensive disease involving pancreatic necrosis and severe inflammation, which can result in multiple organ failure and death (1, 2). Currently, there is no chemotherapeutic drug available for the prevention or treatment of AP.

AP is characterized by aberrant zymogen activation, inflammatory cell infiltration and pancreatic acinar cell death (3). Whereas abnormal trypsinogen activation contributes to the early stages of the disease, activation of the oxidant-sensitive transcription factor nuclear factor-kappaB (NF-κB) in acinar cells is largely responsible for the severe systemic inflammatory response and organ damage (4).

High alcohol intake (> 40 g/day) is a major risk factor for AP (5). Alcoholic pancreatitis is the second leading cause of AP, and the most common cause of chronic pancreatitis (5, 6). Although the mechanism by which chronic alcohol abuse promotes AP is not fully understood, it is generally believed that an intracellular Ca^{2+} overload, as well as the generation of reactive oxygen species (ROS), are the elements responsible for the initiation of the inflammatory process in the gland (7-12). In addition, ethanol enhances cholecystokinin octapeptide (CCK-8)-induced Ca^{2+} overload and ROS generation in pancreatic acinar cells (13-15).

In the pancreas, ethanol is either oxidized to acetaldehyde or esterified with free fatty acids to form free fatty acid ethyl esters (FAEEs). Ethanol oxidation is catalyzed by alcohol dehydrogenase or by cytochrome P450 2E1 (16). The oxidative metabolites of alcohol, notably acetaldehyde, have been suggested as mediators of alcohol-induced organ damage. Because oxidative metabolites are primarily generated in the liver and appear only in extremely low concentrations in the circulation (17, 18), organ damage from acetaldehyde in the pancreas, which shows minimal oxidative ethanol metabolism (19, 20), is considered unlikely. Nonoxidative metabolism of alcohol by esterification with fatty acids has been shown in the pancreas and implicated in the development of pancreatic acinar cell injury (21-23). Some evidences show that ethanol metabolism in the pancreas mainly occurs *via* the nonoxidative pathway and produces FAEEs (24-27). Doyle *et al*. (24) determined the concentration of FAEEs in the blood of 7 healthy human subjects after ethanol intake for a period of up to 24 hours. They found that 7 of 7 samples equivocal for ethanol were positive for FAEEs, suggesting the fatty acid ethyl esters in the blood as markers for ethanol intake. Laposata *et al*. (25, 26) demonstrated that alcohol-intoxicated humans have high levels of FAEEs, in blood, pancreas, and liver, causing pancreatic injury as well as liver damage. Werner *et al*. (27) found that FAEEs at concentrations found in human plasma produce a pancreatitis-like injury in rats, providing direct evidence that FAEEs can produce organ-specific toxicity. Thus, FAEEs may contribute to acute alcohol-induced damage to the pancreas.

The pathogenic mechanism studies for FAEE showed that FAEEs are mainly synthesized and accumulated in pancreatic acinar cells (28) and induce the release of Ca^{2+} from the endoplasmic reticulum (ER), and from zymogen granules by activating inositol triphosphate receptors (29, 30). Ca^{2+} release results in cytoplasmic Ca^{2+} overload and consequently, the activation of digestive enzymes such as trypsinogen, and the initiation of AP. Furthermore, prolonged elevated levels of cytoplasmic Ca^{2+} lead to mitochondrial dysfunction and cell necroptosis (31). The resulting loss of ATP production by damaged mitochondria precludes the restoration of normal Ca^{2+} levels in the ER and cytoplasm by ATP-fueled Ca^{2+} pumps. The formation of free fatty acids *via* inner mitochondrial membrane FAEE hydrolases further limits ATP production by uncoupling oxidative phosphorylation) (30).

Specifically, Ca^{2+} activates NADPH oxidase to produce ROS in pancreatic acinar cells (32), which up-regulate the expression of inflammatory cytokines that contribute to AP (33). Ca^{2+} levels in cultured pancreatic acinar cells are transiently increased by cellular exposure to ethanol in combination with the fatty acid palmitoleic acid, and mice treated with an ethanol and palmitoleic acid cocktail (hereafter referred to as EtOH/POA display increased levels of palmitoleic acid ethyl ester, extensive edema, neutrophil infiltration and acinar cell necrosis (31).

In this study, we used EtOH/POA-treated AR42J cells to examine the inhibition of EtOH/POA-induced Ca^{2+} increases, NADPH oxidase activation, ROS production, mitochondrial function and cell death produced by docosahexaenoic acid (DHA) treatment. Used as a dietary supplement, DHA serves as a powerful anti-oxidant that reduces inflammation (34) and improves the outcomes of patients with AP (35). Necroptosis appears to be necrotic cell death, but finely regulated by a set of intracellular signal transduction pathways (36). Necroptosis is the predominant mode of acinar cell death in severe experimental pancreatitis (37). In our study, activation of necroptosis-regulating proteins such as receptor interacting protein (RIP) and mixed lineage kinase domain-like pseudokinase (MLKL), as necroptosis indices, were measured in AR42J cells treated with EtOH/POA in the presence or absence of DHA. The protective effects of DHA have crucial implications in the prevention or delay of oxidative stress-associated acinar cell necroptosis following exposure to EtOH/POA.

MATERIALS AND METHODS

Reagents

DHA (D2534, ≥ 98%), POA (P9417, ≥ 98.5%), apocynin (PHL83252, ≥ 95%), Nec-1 (480065, ≥ 95%), GSK-872 (5.30389, ≥ 98%), and diclorofluorescein diacetate (DCF-DA, 35845, ≥ 95%) were purchased from Sigma-Aldrich (St. Louis, MO, USA). BAPTA (ab120503, > 97%) was purchased from Abcam (Cambridge, UK). Stock solutions of DHA (1-2 μM) and POA (50 μM) in ethanol were prepared for storage at –20°C. Stock solutions of apocynin (10 μM), Nec-1 (25 μM), BAPTA (5 μM), and GSK-872 (5 μM), were prepared with DMSO.

Cell line and culture conditions

Rat pancreatic acinar AR42J cells (pancreatoma, ATCC CRL 1492) were obtained from the American Type Culture Collection (Manassas, VA, USA) and cultured in Dulbecco's modified Eagle's medium (Sigma, St. Louis, MO, USA) supplemented with 10% fetal bovine serum (GIBCO-BRL, Grand Island, NY, USA) and antibiotics (100 U/mL penicillin and 100 μg/mL streptomycin). The cells were cultured at 37°C in a humidified atmosphere of 95% air and 5% CO_2.

Experimental protocol

To investigate the effect of DHA, the cells (1×10^5 /2 mL) were pre-treated with DHA (1 or 2 μM) for 1 h prior to treatment with EtOH (150 mM) and POA (50 μM) and incubated for 6 h (for cell viability, lactate dehydrogenase (LDH) release, and caspase-3 activity), 15 min (for RIP1, p-RIP1, MLKL, and p-MLKL protein levels), or 10 min (for ROS and adenosine triphosphate (ATP) levels, NADPH oxidase activity, and mitochondrial membrane potential). To determine the involvement of NADPH oxidase in necroptosis, the cells were pre-treated with a NADPH oxidase inhibitor apocynin (10 μM) for 1 h before EtOH/POA stimulation. To determine the role of calcium in necroptosis, cells were treated with the Ca^{2+} chelator BAPTA-AM (5 μM) for 1 h before EtOH/POA stimulation. To detect necroptosis, the cells were pre-treated with the necroptosis inhibitor Nec-1 (25 μM) or the RIP3 inhibitor GSK-872 (5 μM) for 1 h before EtOH/POA stimulation. Control experiments where cells received no treatment ('None') or treatment with EtOH/POA but not DHA ('Control') were performed in parallel.

Prior to the experiments with DHA, apocynin, BAPTA-AM, Nec-1, or GSK-872, time-dependent experiments on intracellular and mitochondrial ROS (for 20 min), cell viability (for 8 h), and levels of necroptosis-regulating proteins such as RIP1, p-RIP1, RIP3, MLKL, and p-MLKL (for 30 min) were performed. In other sets of experiments to determine the effect of ethanol alone and POA alone on intracellular ROS and cell viability, the cells were treated with EtOH (150 mM) alone, POA (50 μM) alone, or EtOH (150 mM) with POA (50 μM) for 10 min (for ROS levels) and 6 h (for cell viability and caspase-3 activity).

To determine the concentration-dependent effects of DHA on EtOH/POA-induced cell death, the cells (1×10^5 /2 mL) were pre-treated with DHA (0.5, 1, or 2 μM) for 1 h prior to treatment with EtOH (150 mM) and POA (50 μM) and incubated for 6 h. Cell viability was determined using the trypan blue exclusion assay.

Preparation of cell extracts

Cell extracts were prepared using a method described by Jeong *et al*. (38). The cells were harvested by scraping with phosphate buffered saline (PBS), and pelleted by centrifugation at 5,000 rpm for 5 min. The cell pellets were resuspended in lysis buffer containing 10 mM Tris (pH 7.4), 1% Nonidet P-40 (NP-40) and a commercial protease inhibitor complex (Complete; Roche, Mannheim, Germany), and lysed by drawing the cells through a 1-mL syringe with several rapid strokes. The mixture was then incubated on ice for 30 min and centrifuged at 13,000 rpm for 15 min. The supernatants were collected and used as whole cell extracts. To prepare cytosolic and membrane extracts, the cells were extracted in homogenization buffer containing 10 mM Tris-HCl (pH 7.4), 50 mM NaCl, 1 mM ethylene diamine tetra-acetic acid (EDTA), and a protease inhibitor complex (Complete; Roche, Mannheim, Germany) and centrifuged at 100,000 × *g* for 1 hour. The pellets were resuspended on ice in lysis buffer containing 50 mM HEPES (pH 7.4), 150 mM NaCl, 1 mM EDTA, and 10% glycerol and used as membrane extracts. The supernatants were used as cytosolic extracts. The protein concentration was determined by the Bradford assay (Bio-Rad Laboratories, Hercules, CA, USA).

Measurement of intracellular and mitochondrial reactive oxygen species levels

Intracellular and mitochondrial ROS levels were measured according to the method described by Kyung *et al*. (39). To measure intracellular ROS levels, the cells were incubated with EtOH/POA and 10 μM DCF-DA (Sigma-Aldrich, St. Louis, MO, USA) for 30 min. Next, the cells were washed and scraped into phosphate-buffered saline (PBS). DCF fluorescence was measured with a Victor5 multi-label counter (PerkinElmer Life and Analytical Sciences, Boston, MA, USA) at excitation and emission wavelengths of 495 nm and 535 nm, respectively. To measure mitochondrial ROS levels, the cells were incubated with EtOH/POA and 10 μM MitoSOX red (M36008, Life Technologies, Grand Island, NY, US) for 30 min. MitoSOX fluorescence was measured with a Victor5 multi-label counter at excitation and emission wavelengths of 514 nm and 585 nm, respectively. ROS levels are expressed as the percentage of the ROS measured in untreated cells ('None').

Determination of cell viability

The cells were plated in a 24-well plate (3×10^4 cells/well) and then cultured overnight. Following the addition of DHA and/or EtOH/POA to the culture, and incubation for a specified period, the number of viable cells remaining was determined using the trypan blue exclusion test (0.2%, trypan blue; Sigma, St. Louis, MO, USA).

Measurement of lactate dehydrogenase release

LDH release was quantified using the LDH Assay kit (ab102526; Abcam, Cambridge, UK). The cells were lysed with lysis buffer containing 0.1M Tris (pH7.4), 10% Triton X-100, and then centrifuged at 10,000 × *g*. LDH activity was measured in culture medium as well as in the cells according to Lopez *et al*. (40). The LDH release is quantified as a percentage compared to the total LDH content (LDH in the supernatant + LDH inside the cells).

Western blot analysis

Western blot analysis was performed using a previously describe method (41). Whole cell extracts (60 – 80 μg protein /lane) were separated using sodium dodecyl sulfate polyacrylamide gel electrophoresis on 10 – 12% acrylamide gels. The proteins were transferred onto nitrocellulose membranes (Amersham, Inc., Arlington Heights, IL, USA) by electroblotting. The transfer of proteins was verified by reversible staining with Ponceau S. Membranes were blocked with 3% non-fat dry milk in Tris-buffered saline and 0.2% Tween 20 (TBS-T) (1 h at room temperature) and then incubated overnight at 4°C with antibodies against receptor-interacting protein (RIP1) (#3493S, Cell Signaling Technology), p-RIP1 (#65746, Cell Signaling Technology), RIP3 (ab62344, Abcam), mixed lineage kinase domain-like pseudokinase (MLKL) (ab183770, Abcam), p-MLKL (ab196436, Abcam), and actin (sc-47778, Santa Cruz Biotechnology, Dallas, TX, USA) in TBS-T containing 3% dry milk. After washing with TBS-T, the primary antibodies were detected using horseradish peroxidase-conjugated secondary antibodies (anti-mouse, anti-rabbit) and an enhanced chemiluminescence detection system (Santa Cruz Biotechnology, Dallas, TX, USA) with exposure to BioMax MR film (Kodak, Rochester, NY, USA).

Measurement of intracellular Ca^{2+}

Intracellular Ca^{2+} was determined using a method described by Zhao *et al*. (42). To measure intracellular Ca^{2+} levels, the cells were seeded on 22 mm × 22 mm glass slides in 35-mm culture dishes and incubated at 37°C in a humidified atmosphere of 95% air and 5% CO_2 overnight. Physiological salt solution containing DHA (2 μM) and fura-2 AM (2 μM) (F1221: Thermo Fisher Scientific) was then added, and following 30 min incubation at room temperature, the cells were washed and incubated with 2 μM DHA in physiological salt solution for 30 min. The cells were then mounted on an inverted microscope (Nikon, Tokyo, Japan). Fluorescence measurements were determined using an imaging system (Molecular Devices, Sunnyvale, CA, USA) and recorded using a charge-couple device camera (CoolSNAP, Tucson, AZ, USA). Fluorescence emission was monitored at 510 nm and reported as the ratio of the respective emission intensity (F340/F380) resulting from 340 nm and 380 nm excitation wavelengths.

In addition, intracellular Ca^{2+} levels were measured using fluo-4 AM, cell permeant (F14201; Thermo Fisher Scientific) (43). The cells were plated in a 96-well plate (4×10^3 cells/well) and then cultured overnight. The cells were loaded with fluo-4 by incubation with HEPES buffer (pH 7.4), containing 1 mM probenecid, 4 μM fluo-4 AM for 1 h at 37°C. Then the cells were treated with or without 2 μM DHA and incubated 1 h at 37°C. The fluorescence was measured using a microplate reader (Molecular Devices, Sunnyvale, CA, USA), at an excitation wavelength of 494 nm and an emission wavelength of 525 nm. Ca^{2+} levels were expressed as $\Delta F/F_0$. F_0 is the resting background fluorescence, ΔF is the fluorescence change over time after treatment with or without EtOH/POA in the presence or the absence of DHA.

Measurement of nicotinamide adenine dinucleotide phosphate oxidase activity

NADPH oxidase activity was measured by using the lucigenin assay (44). Membrane and cytosolic extracts were prepared as described before (38). The assay was performed in 50 mM Tris-MES buffer (pH 7.0) containing 2 mM KCN, 10 μM lucigenin and 100 μM NADPH. The reaction was initiated with the addition of 10 μg of membrane-extract protein. Photon emission was measured using a microplate reader (Molecular Devices, Sunnyvale, CA, USA). For control experiments, cytosolic-extract protein was used in place of membrane-extract protein.

Measurement of caspase-3 activity and adenosine triphosphate level

Caspase-3 activity was quantified using a Caspase-3 Assay Kit according to manufacturer's protocol (ab39383; Abcam). Whole cell extracts were prepared as described earlier (38) and mixed with buffer containing a colorimetric substrate for caspase-3 (N-acetyl-Asp-Glu-Val-Asp p-nitroanilide). The mixtures were incubated for 1 h at 37°C before measuring the optical density at 405 nm with a microplate reader. ATP levels in whole cell extracts were measured using a Luminescent ATP Detection Assay Kit according to the manufacture's protocol (ab113849; Abcam).

Measurement of mitochondrial membrane potential (MMP)

Mitochondrial depolarization was monitored by treating cells with the fluorescent dye 5,5',6,6'-tetrachloro-1,1',3,3'-tetraethyl benzimidazolyl carbocyanine iodide (JC-1) and measuring the intensity of red emission relative to the intensity of green emission (45). Mitochondrial depolarization is indicated by a decrease in the red/green fluorescence intensity ratio. To determine changes in MMP, cells cultured on glass coverslips were treated with DHA for 2 h and then with EtOH/POA for 10 min, before incubating them with JC-1 reagent (1:100 dilution; 10009908, Cayman Chemical Company, Ann Arbor, MI, USA) for 20 min. After removing the medium, the cells were dried for 15 min at room temperature and washed twice with PBS for 5 min. The cells were then mounted with mounting solution (M-7534, Sigma Aldrich). JC-1 fluorescence (red; excitation at 590 nm and emission at 610 nm, green; excitation at 485 nm and emission at 535 nm) was measured with a laser-scanning confocal microscope (LSM 880, Carl Zeiss Inc, Oberkochen, Germany). Fluorescent images were used in conjunction with NIH Image J 5.0 software (National Institutes of Health, Bethesda, MD, USA) to determine the percentage ratio of red and green fluorescence intensities. The average intensity per cell was calculated for each experimental group comprised of more than 50 cells.

Statistical analysis

All experimental values are expressed as the mean ± standard error (SE) of three different experiments. Analysis of variance (ANOVA), followed by the Newman-Keul's *post hoc* test was used for the statistical analysis. A P-value of 0.05 or less was considered statistically significant.

RESULTS

EtOH/POA increases reactive oxygen species levels and induces RIP1-dependent cell death

To determine the effect of EtOH/POA on ROS production in AR42J cells, intracellular and mitochondrial ROS levels were measured following 5 – 20 min-incubation periods. As shown in *Fig. 1A* and *1C*, the maximum increases in intracellular (~1.5-fold) and mitochondrial ROS (~3-fold) levels occur within 10 min of exposure of the cells to EtOH/POA. However, treatment of EtOH alone or POA alone had no effect on ROS levels in

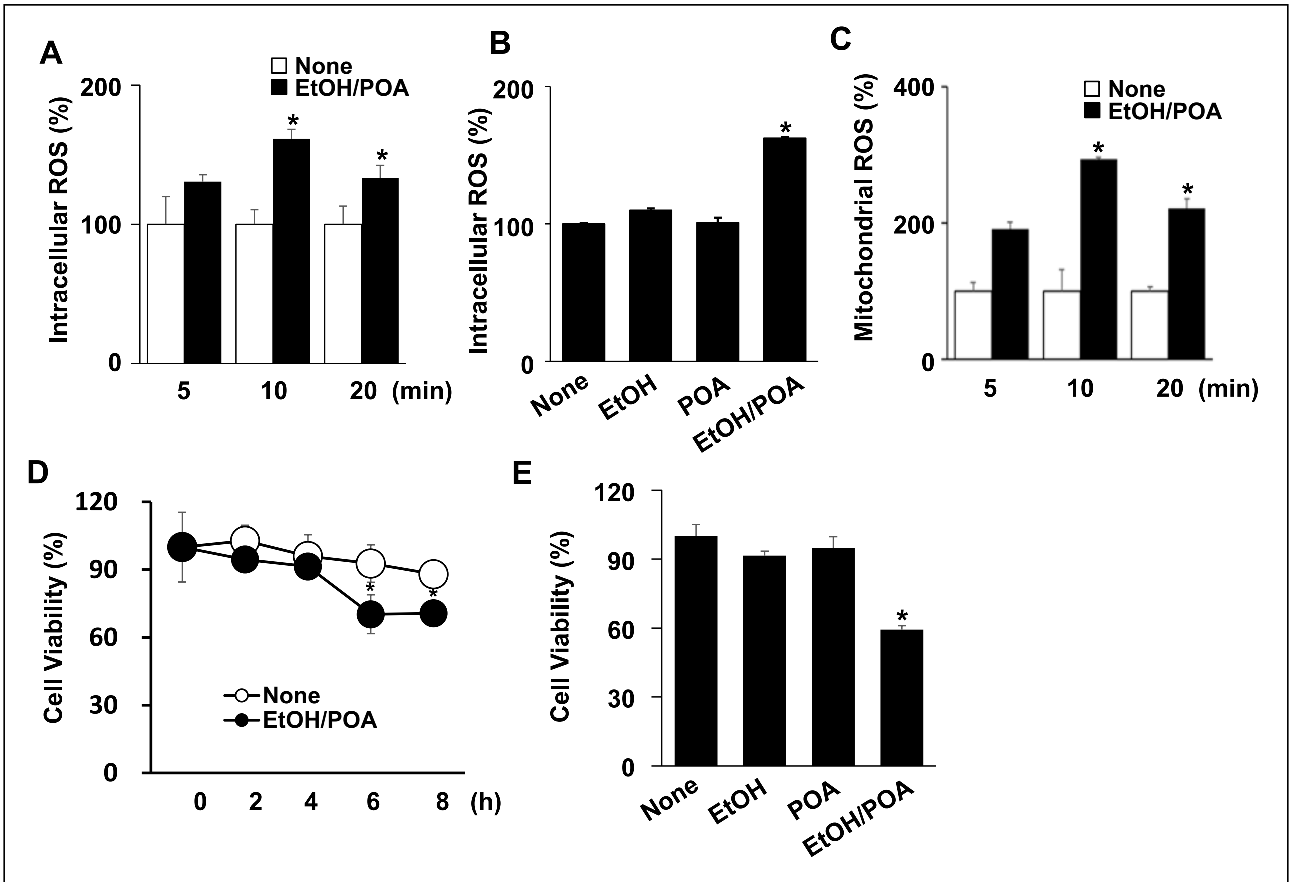

Fig. 1. The effect of EtOH/POA on ROS production and cell viability in AR42J cells. (A, B, C): Comparison of the levels of intracellular and mitochondrial ROS measured for untreated cells ('None') and for cells incubated with 150 mM EtOH and 50 µM POA for the indicated time periods ('EtOH/POA'). *P < 0.05 versus the corresponsding 'None'. (D): Comparison of the cell viability, accessed periodically over an 8 h period, for cell cultures incubated with and without 150 mM EtOH and 50 µM POA. *P < 0.05 versus the corresponsding 'None'. (E): Comparison of the cell viability at 6 h for cell cultures incubated with 150 mM EtOH alone, 50 µM POA alone or 150 mM EtOH/50 µM POA. *P < 0.05 versus the corresponsding 'None'.

AR42J cells after 10 min of culturing (*Fig. 1B*). This result indicates that FAEE produced by EtOH and POA may stimulate ROS production.

To examine the effect of EtOH/POA on AR42J cell viability, cell cultures were treated with EtOH/POA for up to 8 hours. The viable cell number was measured periodically using the trypan blue exclusion test. *Fig. 1D* shows that at 6 h, cell viability decreased by ~25%. However, EtOH alone and POA alone had no effects on cell viability at 6-h (*Fig. 1E*). To investigate if the decreased number of viable cells is the result of EtOH/POA-induced necroptosis, we first determined the impact of EtOH/POA on cellular levels of the necroptosis-signaling pathway proteins RIP1, RIP3, and MLKL. Western blot analysis (*Fig. 2A*) shows that exposure of the AR42J cells to EtOH/POA for 15 min results in a significant increase in the phospho-specific forms of RIP1 and MLKL. Moreover, RIP3 increased following treatment with EtOH/POA in a time-dependent manner. However, EtOH/POA did not increase caspase-3 activity in AR42J cells (*Fig. 2B*). Next, we tested whether the necroptosis inhibitor necrostatin (Nec-1) and RIP3 inhibitor GSK-872 reduces the magnitude of the EtOH/POA-induced decreases in cell viability. Cultures treated with Nec-1 and GSK-872 retained more cells following incubation with EtOH/POA than did the control (EtOH/POA alone) (*Fig. 2C* and *2D*). In comparison, the increased cell retention of cultures treated with the apoptosis inhibitor Z-VAD-fmk before incubation with EtOH/POA was found to be considerably smaller (*Fig. 2C*). Taken together, EtOH/POA induces AR42J cell death primarily *via* the necroptotic pathway.

Apocynin and BAPTA inhibit EtOH/POA-induced increases in reactive oxygen species and necroptotic pathway proteins RIP1 and MLKL

Because NADPH oxidase and Ca^{2+}-signaling are known to play key roles in ROS production, our next step was to measure the impact of the NADPH oxidase inhibitor apocynin and Ca^{2+} chelator BAPTA on EtOH/POA-induced increases in ROS and cell death. For this purpose, we first measured intracellular and mitochondrial ROS production in AR42J cells treated with EtOH/POA in the presence or absence of these inhibitors. The results in *Fig. 3A* and *3B* show that apocynin and BAPTA reduce intracellular and mitochondrial ROS levels in the EtOH/POA-treated cells.

Next, we tested the effect of 10 µM of the NADPH oxidase inhibitor apocynin or 5 µM of the Ca^{2+} chelator BAPTA on the EtOH/POA-induced increase in NADPH oxidase activity in membrane extracts from AR42J cells. As shown in *Fig. 3C*, both apocynin and BAPTA inhibited EtOH/POA-induced increases in NADPH oxidase activity in AR42J cells. We also found that the observed EtOH/POA-induced increases in the levels of phosphophorylated forms of RIP1 and MLK are suppressed by pre-treatment of the cells with apocynin or BAPTA (*Fig. 3D*). Moreover, by measuring cell viability in cultures treated with EtOH/POA in the presence and absence of the respective inhibitors, we discovered that EtOH/POA-induced cell death is also reduced (*Fig. 3E*). These results indicate that EtOH/POA increases ROS levels and necroptotic AR42J cell death by promoting Ca^{2+} overload and NADPH oxidase activation.

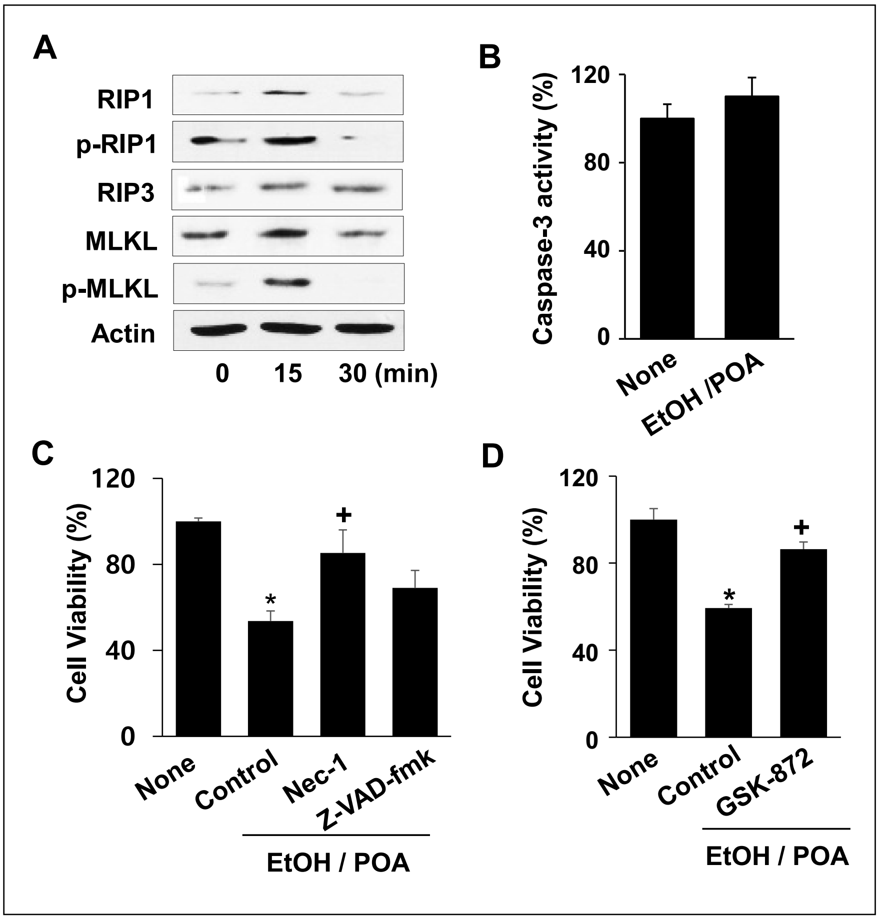

Fig. 2. The effect of Nec-1, z-VAD-fmk and GSJ-872 on EtOH/POA-induecd cell death in AR42J cells. (A): Western blot analysis of phospho-specific and total forms of R1P1 and MLKL in untreated AR42J cells ('0' min) and cells treated with 150 mM EtOH and 50 µM POA for 15 and 30 min. Actin was used as the loading control. (B): A comparison of caspase-3 acvitity for untreated cells ('None') and for cells incubated with 150 mM EtOH and 50 µM POA for 6 h. (C): A comparison of the cell viability measured for untreated cell cultures ('None') and for cell cultures incubated with (or without, 'Control') 25 µM necroptosis inhibitor Nec-1 or 10 µM apoptosis inhibitor Z-VAD-fmk for 1 h, and then incubated for 6 h with 150 mM EtOH and 50 µM POA. (D): Comparison of the cell viability measured for untreated cell cultures ('None') and for cell cultures incubated with (or without, 'Control') 5 µM RIP3 inhibitor GSK-872 for 1 h, and then incubated for 6 h with 150 mM EtOH and 50 µM POA. *P < 0.05 versus None; +P < 0.05 versus Control.

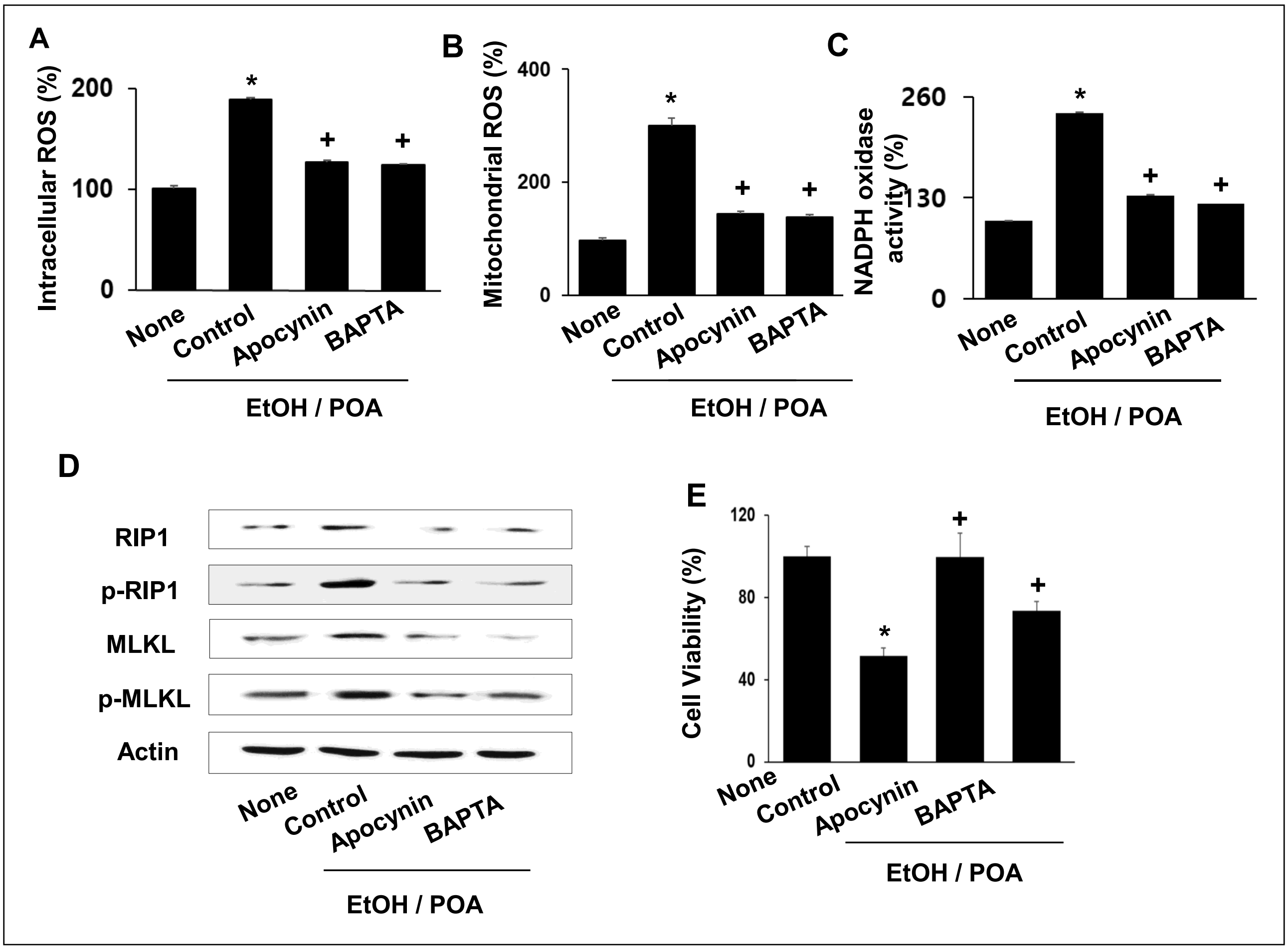

Fig. 3. Determination of the effect of apocynin and BAPTA on EtOH/POA-induced alteration of ROS production, NADPH oxidase activity, necroptotic signal transduction pathway proteins and cell viability in AR42J cells. (A, B): Comparison of the levels of intracellular and mitochondrial ROS measured for untreated cells ('None') and for cells incubated without ('Control') or with 10 µM NADPH oxidase inhibitor apocynin or 5 µM Ca^{2+} chelator BAPTA for 1 h and then with 150 mM EtOH and 50 µM POA for 10 min. *P < 0.05 versus None; +P < 0.05 versus Control. (C): NADPH oxidase activity in untreated cells ('None') and in cells incubated without ('Control') or with 10 µM apocynin or 5 µM BAPTA for 1 h and then incubated with 150 mM EtOH and 50 µM POA for 10 min. *P < 0.05 versus None; +P < 0.05 versus Control. (D): Western blot analysis of phospho-specific and total forms of R1P1 and MLKL in cells treated as reported in (C) except that a 15 min EtOH/POA incubation period was used. Actin was used as the loading control. (E): Comparison of the cell viability measured for untreated cells ('None') and for cells incubated without ('Control') or with 10 µM apocynin or 5 µM BAPTA for 1 h and then with 150 mM EtOH and 50 µM POA for 6 h. *P < 0.05 versus None; +P < 0.05 versus Control.

Docosahexaenoic acid inhibits EtOH/POA-induced increases in reactive oxygen species levels, nicotinamide adenine dinucleotide phosphate oxidase activity, and necroptosis

To determine if DHA protects AR42J cells from EtOH/POA-induced oxidative stress, the effect of DHA on the levels of ROS and NADPH oxidase in EtOH/POA-treated cells was measured. At a concentration of 2 µM, DHA almost fully suppresses the EtOH/POA-induced increases in intracellular (*Fig. 4A*) and mitochondrial (*Fig. 4B*) ROS levels and NADPH oxidase activity (*Fig. 4C*). We also found that DHA suppresses EtOH/POA-induced increases in phosphor-specific forms of RIP1 and MLKL (*Fig. 5A*) and the loss of cell viability (*Fig. 5B*) in a concentration-dependent manner.

The major feature of necrotic cells is plasma membrane permeabilization. This event can be observed by measuring LDH release. LDH is a cytoplasmic enzyme that is released into the extracellular space when the plasma membrane is damaged (46). As shown in *Fig. 5C*, EtOH/POA increased LDH release. DHA inhibited EtOH/POA-induced leakage of LDH. This result indicates that DHA suppressed EtOH/POA-induced necrotic cell death. Conversely, the effect of EtOH/POA (with or without DHA) on caspase-3 is comparatively small (*Fig. 5D*). Because increased caspase-3 activity is a marker for apoptosis, this result suggests that EtOH/POA-induced cell death appears to occur primarily *via* the necroptosis pathway, consistent with the observation of the greater restorative effect of Nec-1 and GSK-872 on cell viability compared to that of Z-VAD-fmk (*Fig. 2C* and *2D*).

Docosahexaenoic acid does not inhibit EtOH/POA-induced increases in Ca^{2+} *oscillation and levels in AR42J cells*

We found that the calcium Ca^{2+} chelator BAPTA inhibited EtOH/POA-induced increases in NADPH oxidase activity in AR42J cells (*Fig. 3C*). These results indicate that Ca^{2+} may

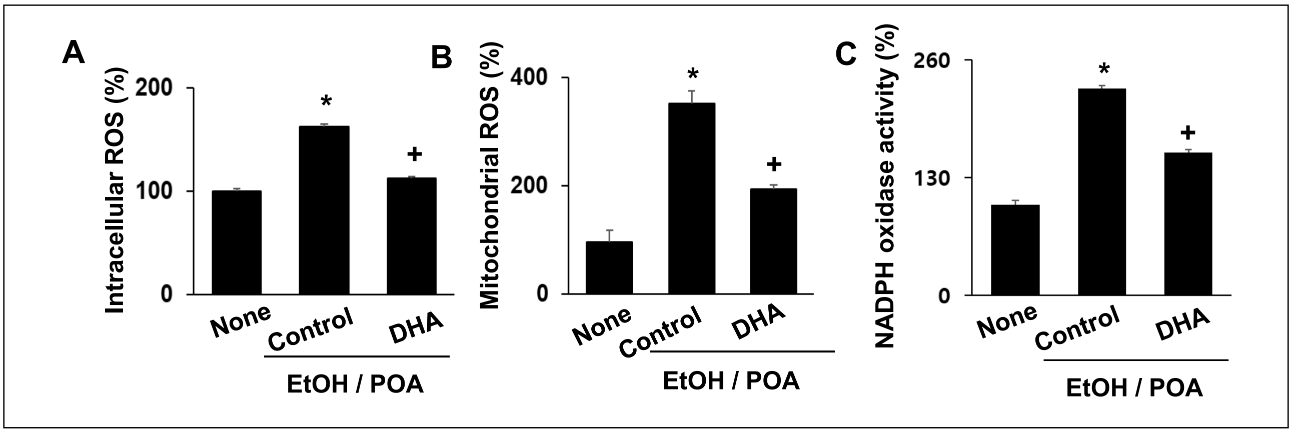

Fig. 4. Determination of the effect of DHA on EtOH/POA-induced alteration of ROS production and NADPH oxidase activity in AR42J cells. (A, B): Comparison of the levels of intracellular and mitochondrial ROS measured for untreated cells ('None') and for cells incubated without ('Control') or with 2 μM DHA for 1 h and then with 150 mM EtOH and 50 μM POA for 10 min. *P < 0.05 versus None; +P < 0.05 versus Control. (C): Comparison of NADPH oxidase activity in cells treated as reported in (A, B). *P < 0.05 versus None; +P < 0.05 versus Control.

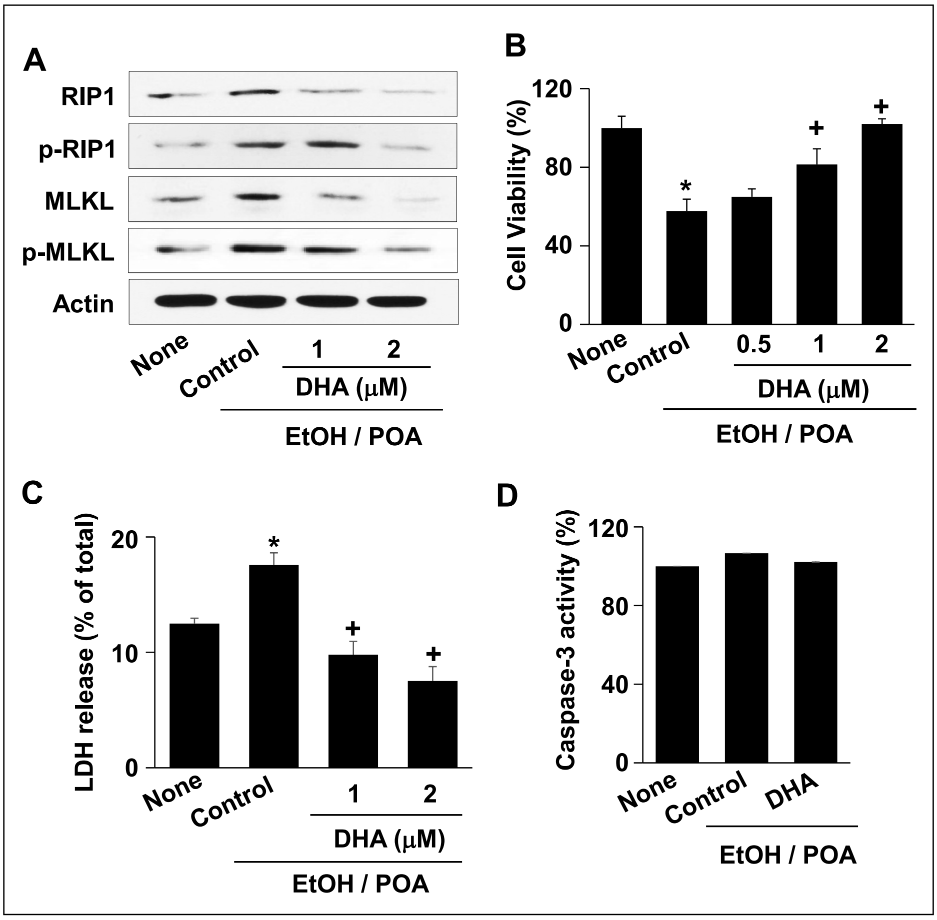

Fig. 5. Determination of the effect of DHA on EtOH/POA-induced alteration of necroptotic signal transduction pathway proteins, cell viability, LDH release and caspase-3 activity in AR42J cells. (A): Western blot analysis of phospho-specific and total forms of R1P1 and MLKL in untreated cells ('None') and for cells incubated without ('Control') or with 1 or 2 μM DHA for 1 h, and then with 150 mM EtOH and 50 μM POA for 15 min (B, C): Comparison of the cell viability and LDH release measured for untreated cells ('None') and for cells incubated without ('Control') or with the indicated concentration of DHA for 1 h and then with 150 mM EtOH and 50 μM POA for 6 h. *P < 0.05 versus None; +P < 0.05 versus Control. (D): Comparison of caspase-3 activity measured for cells treated as is reported in (A, B) except that the EtOH/POA incubation was carried out for 6 h. *P < 0.05 versus None; +P < 0.05 versus Control.

mediate activation of NADPH oxidase in EtOH/POA-treated cells. DHA suppressed EtOH/POA-induced activation of NADPH oxidase in AR42J cells (*Fig. 4C*). Thus, our next step was to examine whether EtOH/POA increases intracellular Ca^{2+} oscillation and levels and whether DHA inhibits EtOH/POA-induced increases in intracellular Ca^{2+} oscillation (*Fig. 6A*) and levels (*Fig. 6B*) in AR42J cells.

Accordingly, Ca^{2+} oscillation in AR42J cells treated with EtOH/POA in the presence and absence of DHA was monitored by fluorescence imaging with the intracellular Ca^{2+} indicator fura-2 AM. As shown in *Fig. 6A*, EtOH/POA increased Ca^{2+} oscillation in the cells. Ca^{2+} oscillation consisted of an initial increase followed by a decrease of intracellular Ca^{2+} towards a value close to the pre-stimulation level. Our results were supported by the study of Fernandez-Sanchez *et al.* (13) showing that acute ethanol exposure on CCK-8-evoked intracellular Ca^{2+} signals in mouse pancreatic acinar cells, determined using fura-2 AM. As shown in *Fig.*

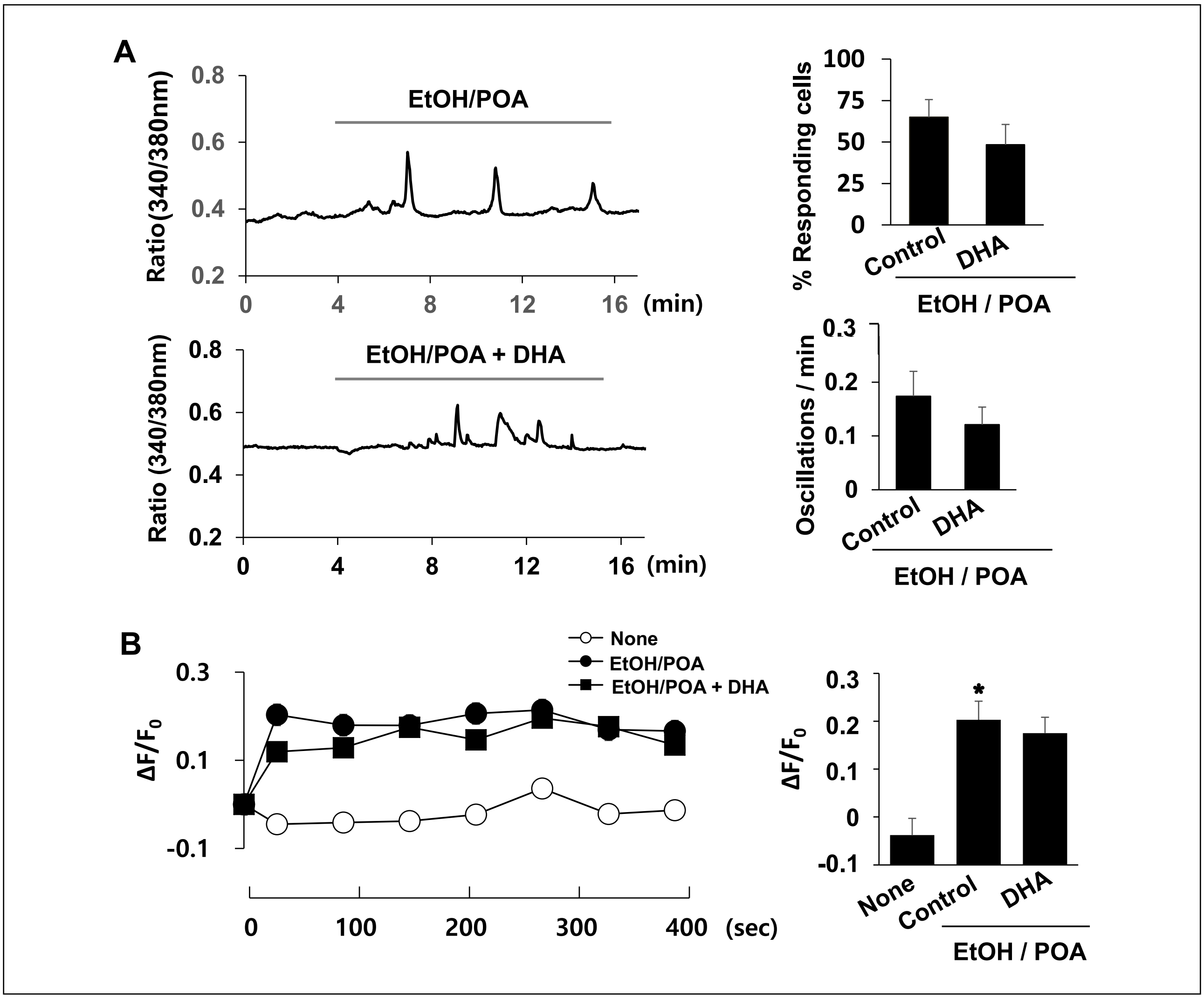

Fig. 6. Determination of the effects of EtOH/POA and DHA on intracellular Ca^{2+} oscillation and levels in AR42J cells using the intracellular Ca^{2+} indicators fura-2 AM and fluo-4 AM fluorescent dyes. (A): The changes in intracellular Ca^{2+} levels in response to cell incubation with 150 mM EtOH and 50 μM POA in the absence (top panel) or presence (bottom panel) of DHA (2 μM). Ca^{2+} level was reported as the ratio fura-2-derived fluorescence emission intensities measured at 510 nm and resulting from excitation at 340 nm and 380 nm (F340/380). Right panels: The percentage of responding cells (top panel) and the Ca^{2+} oscillation frequency (oscillations/min) (bottom panel). (B): The fluorescence transient changes in response to cell incubation with 150 mM EtOH and 50 μM POA in the absence or presence of DHA (2 μM). Ca^{2+} level was reported as the fluorescence changes measuring fluoro-4-derived fluorescence using excitation wavelength of 494 nm and emission wavelength of 525 nm. Ca^{2+} levels were expressed as $\Delta F/F_0$. F_0 is the resting background fluorescence, ΔF is fluorescence change with time after treatment with or without EtOH/POA in the presence or the absence of DHA. Fluorescence transient changes (obtained within 1 – 3 min) were plotted (left panel). (Right panels): Ca^{2+} levels, expressed as $\Delta F/F_0$, of the cells. *P < 0.05 versus None.

5A, EtOH/POA increased Ca^{2+} oscillation in the cells. EtOH/POA treatment with DHA (2 μM) showed a similar Ca^{2+} oscillation to that observed for cells without DHA treatment.

Ca^{2+} levels in AR42J cells treated with EtOH/POA in the presence and absence of DHA (2 μM) was monitored by transient fluorescence changes using the intracellular Ca^{2+} indicator fluo-4 AM. Transient fluorescence changes (obtained within 1-3 min) were plotted. Ca^{2+} levels, expressed as $\Delta F/F_0$, were increased by EtOH/POA. However, DHA did not reduce EtOH/POA-induced increases in Ca^{2+} levels in AR42J cells (*Fig. 6B*). Taken together, DHA did not reduce EtOH/POA-induced increases in Ca^{2+} oscillation and levels in AR42J cells.

Docosahexaenoic acid inhibits EtOH/POA-induced mitochondrial dysfunction in AR42J cells

Because elevated ROS production such as that observed for EtOH/POA-treated AR42J cells (*Fig. 1A* and *1C*) can potentially damage mitochondria, our next step was to determine the effect of EtOH/POA (with and without DHA) on mitochondrial membrane potential (MMP) and ATP production. *Fig. 7A* and *7B* show that EtOH/POA treatment reduces both MMP and ATP production, and that DHA pretreatment boosts ATP levels and reduces loss of MPP in EtOH/POA-treated cells. These results indicate that DHA protects against EtOH/POA-induced mitochondrial dysfunction, which may occur *via* DHA-mediated reduction in ROS.

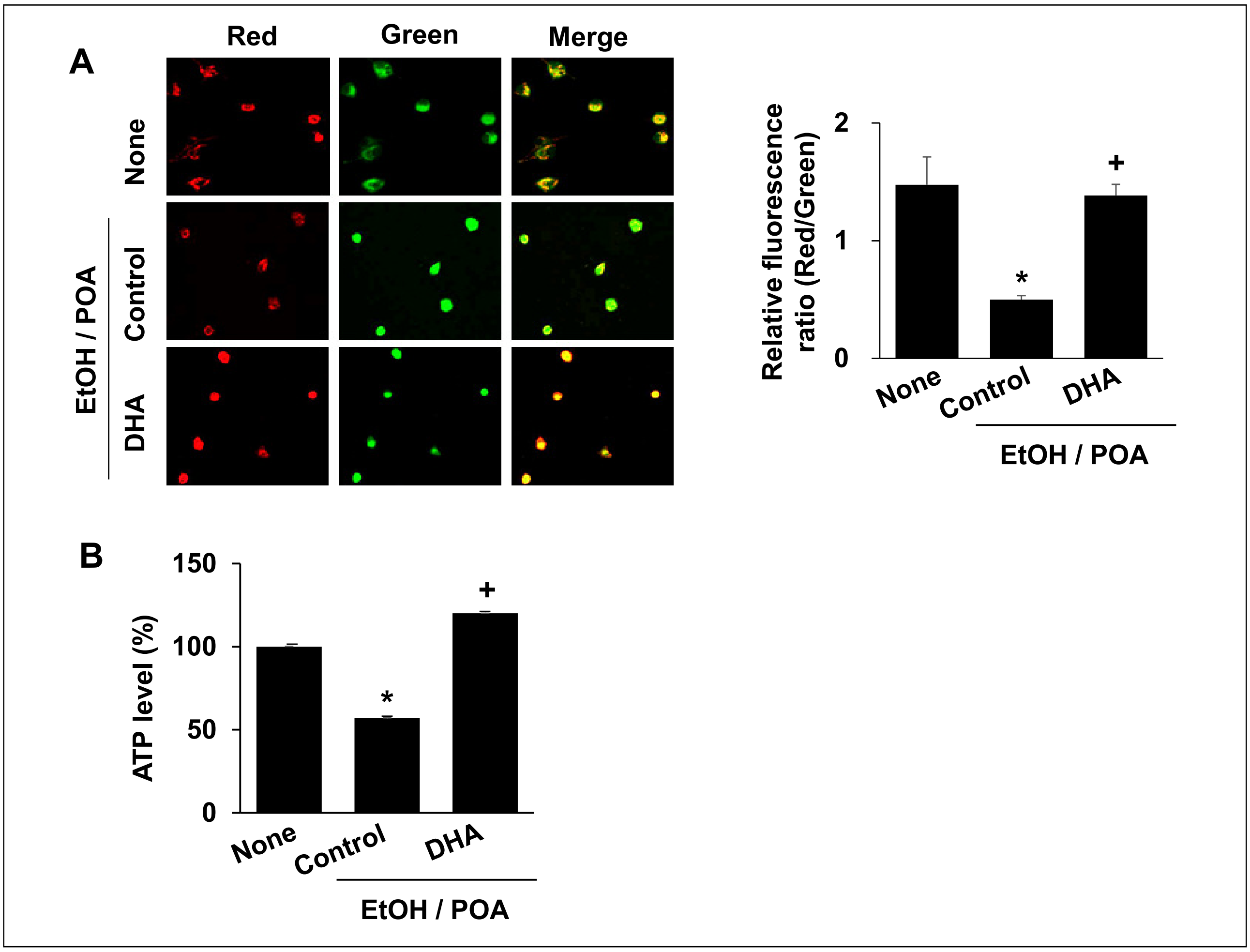

Fig. 7. DHA inhibition of EtOH/POA-induced mitochondrial dysfunction in AR42J cells. Cells were incubated with 2 μM DHA or vehicle ('Control') for 1 h and then with 150 mM EtOH and 50 μM POA for 10 min. 'None' refers to untreated cells. (A): Determination of mitochondrial membrane potential. Left panel: Photomicrographs of JC-1-stained cells showing green and red emissions. Right panel: The ratio of red to green fluorescence emission intensities measured for treated and untreated cells. $^{*}P < 0.05$ versus None; $^{+}P < 0.05$ versus Control. (B): The relative levels of intracellular ATP measured with the luciferase-based assay. $^{*}P < 0.05$ versus None; $^{+}P < 0.05$ versus Control.

DISCUSSION

This study was performed to gain insight into the molecular mechanism by which the omega-3 fatty acid DHA administered to patients suffering from AP improves disease outcomes. Because acinar cells perform the exocrine functions of the pancreas and are key players in AP, they are used for *in vitro* studies of the disease. Recent studies have validated the use of rodent pancreatic acinar cells in place of human pancreatic acinar cells (47) and thus, our studies were performed using rat pancreatic acinar AR42J cells as the experimental platform. Given that alcohol abuse is a major cause of AP (48), and that FAEEs derived from the esterification of ethanol by endogenous free fatty acids are the mediators (31, 49), we used a cocktail (viz. EtOH/POA) of ethanol and palmitoleic acid to simulate the *in vitro* effects of ethanol abuse in AR42J cell cultures.

Inflammation and the associated overproduction of ROS are key traits of alcoholic pancreatitis (50). Experimentally, pancreatic acinar cells subjected to chemically induced stress respond by increasing ROS production (51-55). To examine the effect of EtOH/POA on AR42J cells, we measured the levels of intracellular and mitochondrial ROS and observed that EtOH/POA increases ROS production while it decreases cell viability (*Fig. 1A-1C*). Importantly, these effects are attenuated in cells pre-treated with DHA (*Fig. 4A*, *4B* and 4*E*). Thus, DHA is effective in blocking the formation of toxic levels of ROS induced by the EtOH/POA.

Necrosis is recognized as the major form of pancreatic cell death that occurs during AP. Necroptosis, which is the most well-understood form of necrosis (37), is initiated by pro-inflammatory cytokine tumor necrosis factor-alpha (TNF-α) and is mediated by the signaling kinases RIP and MLKL. RIP1 activation *via* autophosphorylation leads to activation of RIP3 and hence, MLKL activation by phosphorylation (56-58). MLKL activation triggers necroptotic cell death. To test whether EtOH/POA-induced cell death is mediated *via* the necroptosis signal transduction pathway, we measured the levels of phosphorylated and total RIP1 and MLKL. EtOH/POA treatment increased the phosphorylated forms of RIP1 and MLKL (*Fig. 2A*). Furthermore, by employing the necroptosis inhibitor necrostatin-1 (Nec-1) to inhibit necroptosis-promoting RIP1 kinase activity and Z-VAD-fmk to inhibit apoptosis-promoting caspase activity, we showed that EtOH/POA-induced cell death occurs primarily by necroptosis (*Fig. 2C*). This conclusion is further supported by the observation that the apoptotic marker caspase-3 is not impacted by cell treatment with EtOH/POA (*Fig. 4F*).

ROS formation is catalyzed by the membrane-bound enzyme complex NADPH oxidase. NADPH oxidase is believed to play a central role in the pathogenesis of pancreatitis (59). We observed that AR42J cells responded to EtOH/POA by increasing the level of active NADPH oxidase (*Fig. 3C*), consistent with the EtOH/POA-induced increase observed in intracellular and mitochondrial ROS. Pre-treatment of AR42J cells with the NADPH oxidase inhibitor apocynin reduced EtOH/POA-induced increases in NADPH oxidase activity, ROS formation, phosphorylation of RIP1 and MLKL, and cell death (*Fig. 3*). These findings suggest that EtOH/POA-induced cell death results from increased NADPH oxidase activity.

Previous studies have revealed the interplay between NADPH oxidase activity and intracellular Ca^{2+} overload (60). ER-stored Ca^{2+} is transiently released into the cytoplasm through the activation of ER membrane Ca^{2+} channels. In our study we used the Ca^{2+}-specific chelator BAPTA to reveal that the EtOH/POA-induced increase in NADPH oxidase activity is Ca^{2+}-mediated (*Fig. 3C*). Moreover, BAPTA blocked the effects of EtOH/POA on intracellular and mitochondrial ROS production (*Fig. 3A* and *3C*), phosphorylation of RIP1 and MLKL (*Fig. 3D*) and cell death (*Fig. 3E*) as well. Importantly, pre-treatment of AR42J cells with DHA attenuated the effects of EtOH/POA on NADPH oxidase activity, and downstream processes. However, EtOH/POA-induced, intracellular Ca^{2+}-oscillation was not affected by DHA (*Fig. 5*). Even though DHA had no effect on Ca^{2+}-oscillation, it inhibits NADPH oxidase activity which induces ROS-mediated necroptosis in AR42J cells exposed to the EtOH/POA.

Lastly, we examined the effects of EtOH/POA and DHA on mitochondrial function. Mitochondria are the major source of ROS. When ROS levels exceed antioxidant enzyme capacity they are damaged and undergo loss of membrane polarization and the ability to supply the cell with ATP (61, 62). Moreover, FAEEs bind to and accumulate within the inner mitochondrial membrane, uncoupling oxidative phosphorylation causing a loss of membrane polarization and ATP synthesis (63). The observed EtOH/POA-induced increase in intracellular and mitochondrial ROS (*Fig. 1A* and *1B*) is accompanied by a significant loss in MPP and ATP level (*Fig. 6*). AR42J cells pre-treated with DHA displayed significantly less mitochondrial dysfunction (*Fig. 6*), thus underscoring the protective effect of DHA.

Regarding FAEE toxicity, several studies reported that nonoxidative metabolites of ethanol such as FAEE accumulate in higher concentrations in the pancreas than in other organs after ethanol consumption in human (26) and rats (64, 65). Administration of FAEEs to rats causes pancreatic damage in experimental models of pancreatitis (27). However, ethanol alone and the oxidative metabolite acetaldehyde have minimal or no effects on damage of pancreatic acinar cells, whereas the FAEE induces in acinar cell necrosis (65, 66). Criddle *et al*. (66) demonstrated that freshly isolated pancreatic acinar cells, from the pancreas of adult CD1 mice by using collagenase, exposed to ethanol (up to 850 mM) showed little or no increase in intracellular Ca^{2+}. The oxidative metabolite acetaldehyde (up to 5 mM) had no effect, whereas the nonoxidative unsaturated metabolite palmitoleic acid ethyl ester (10 – 100 μM, added on top of 850 mM ethanol) induced sustained, concentration-dependent increases in intracellular Ca^{2+} that were acutely dependent on external Ca^{2+} and caused cell death. They concluded that nonoxidative fatty acid metabolites, rather than ethanol itself, are responsible for the marked elevations of intracellular Ca^{2+} that mediate toxicity in the pancreatic acinar cells and that these compounds act primarily by releasing Ca^{2+} from the endoplasmic reticulum. Siech and Letko (67) showed that 180 mM ethanol alone had no statistically significant effect on cell survival at 4 h-incubation periods using freshly isolated pancreatic acinar cells from female albino rats. In this study, 150 mM ethanol alone did not affect cell viability (*Fig. 1B)*, which was in agreement of the studies by Criddle *et al* (66) and Sieh and Letko (67).

Criddle *et al*. (66) also demonstrated that 50 μM POA induces sustained Ca^{2+} release and increased cell death with treatment of ethanol from 50 – 850 mM. They found that ethanol/POA-induced cell death is Ca^{2+}-dependent necrosis. This study supports the present results showing that 150 mM ethanol/50 μM POA increased Ca^{2+} release and induced necroptosis in AR42J cells.

Other studies using cancer cell lines, macrophage, and primary hepatocytes, the concentrations of ethanol ranging from 2.5% to 0.15% concentration were well-tolerated by cells with respect to proliferation. Ethanol is a good choice for solvent since it has low toxicity on human liver cancer *cell* line HepG2, human breast cancer cell lines (MDA-MB-231, MCF-7) and Vietnamese breast cancer stem cell (*VNBRCA1)* (68). 24-h treatment of ethanol (0.5%) had little or no toxicity in MCF-7, murine macrophage RAW-264.7 and human umbilical vein endothelial cells (HUVEC) (69). In freshly isolated hepatocytes from male Wistar rat liver, 5% ethanol did not induce cytotoxicity while 10% ethanol showed cytotoxic effect at 1 h-culture (70).

For the determination of FAEE, Werner *et al*. (64) evaluated whether ethanol-induced pancreatic injury is related to the level of FAEE generated. The animals were allocated to four groups that received ethanol (varying concentrations: 2.5% (0.4 g/kg), 5% (0.8 g/kg), 10% (1.6 g/kg), and 20% (3.2 g/kg)). Two hours after a 2-ml bolus and 6-ml infusion of 2.5% (0.4 g/kg) ethanol did not induce pancreatic edema or trypsinogen activation in pancreatic tissues. However, both parameters increased with doses of 5% ethanol (0.8 g/kg) or greater. FAEE concentration in pancreas was evaluated by gas chromatography-mass spectroscopy (GC-MS) after the start of ethanol infusion (2-ml bolus at 0.8 g/kg; and 6-ml infusion over 2 h at 1.2 g/kg/h). FAEE concentration of pancreatic tissue was about 150 nmol/g tissue. FAEE concentration of rat pancreatic homogenates incubated with 50 mM ethanol was 200 nmol/g tissue at 1 h-incubation (65). Since FAEE produced by ethanol treatment was relatively low, FAEE concentration can be determined using GC-MS in lipid extracts of the cells. FAEE was isolated from the organic phase by solid phase and concentrated by drying the samples under nitrogen. FAEE were then quantitated by GC-MS analysis on a GC coupled to MS (64, 65). Since determination of the exact concentration of FAEE generated from treatment of EtOH/POA is important, it is necessary to determine FAEE concentration in this system for the further study with collaboration of the specialists in GC-MS analysis.

In regard to the concentration of DHA, treatment with DHA at 0.1 and 1 μM significantly inhibited the decrease in cell viability induced by H_2O_2 in retinal ganglion cells (71). 1 μM DHA inhibited hydrogen peroxide-induced cell death in neural progenitor cells (72). Previously, we showed that DHA (5 μM) inhibited hydrogen peroxide-induced cell death and DNA fragmentation and increases in Bax and p53 in AR42J cells (73). Therefore, we used DHA (1 or 2 μM for inhibitory mechanism of DHA in ethanol (150 mM)/POA (50 μM)-induced cell death using AR42J cells.

In the present study, we used AR42J cells which derive initially from a transplantable tumour of a rat exocrine pancreas (74). This is the only cell line currently available that, in culture, maintains many characteristics of normal pancreatic acinar cells, such as Ca^{2+} signalling, the synthesis and secretion of digestive enzymes, protein expression, growth and proliferation (75, 76). AR42J cell receptor expression and signal transduction mechanisms parallel those of pancreatic acinar cells. Thus, this cell line has been widely used as an '*in vitro*' model to study acinar cell function (77).

Logsdon *et al*. (78) demonstrated that glucocorticoids increased the volume density of secretory granule and the synthesis, cell content, and mRNA levels of amylase in AR42J cells. They also found that dexamethasone increased cholecystokinin receptors and amylase secretion in AR42J cells (79). Rajasekaran *et al*. (80) demonstrated that treatment with 10 nM dexamethasone resulted in a 4.6-fold increase in the secreted amylase activity by a reorganization of the RER from a tubulo-vesicular (TV-RER) to a stacked cisternal (SC-RER) configuration in AR42J cells. They suggested that SC-RER is a biosynthetically more efficient form of the RER, which is found predominantly in actively secreting cells. In the present study, we did not determine exocrine function of AR42J cells and determined the EtOH/POA-mediated cell death. Since EtOH/POA induces intracellular Ca^{2+} which activates amylase release, AR42J cells treated with dexamethasome might be useful for determining the effect of DHA on EtOH/POA-induced alterations in exocrine function in relation to alcoholic pancreatitis.

Human pancreatic acinar cells were isolated from pancreatic tissues obtained from aborted foetus (C35 weeks) by autopsy (81), human pancreatic tissue devoid of islets of Langerhans, from dead organ donors without morphological or histological evidence of pancreatic disease (47, 82), or specimens of normal human pancreas obtained from the patients undergoing resection of pancreatic tumors (83). At present, human primary pancreatic acinar cells are not commercially available. Therefore, freshly isolated pancreatic acinar cells from mice or rats may be useful to determine the inhibitory effect of DHA on EtOH/POA-induced pancreatic damage for the further study.

It have been well known that NADPH oxidase and ROS participate in the regulation of necroptosis and the function of ROS in necroptosis is to enhance necrosome formation (84-89). However, some studies reported that activated RIP1 or RIP3 can promote ROS production (90, 91). In present study, ROS production was followed by activation of RIP1 in EtOH/POA-stimulated cells. Inhibition of NADPH oxidase using apocynin suppressed activation of RIP1 in EtOH/POA-stimulated cells. These results indicate that ROS mediate RIP1 activation and necroptosis. Since DHA inhibit ETOH/POA-induced activation of NADPH oxidase, DHA may recue ROS and subsequently suppress activation of necroptosis-regulating proteins (RIP, MLK) in AR42J cells. However, it may be possible that DHA may directly inhibit necroptosis in ROS-independent manner. Further study should be performed to determine whether DHA inhibits necroptosis in ROS-independent way in AR42J cells exposed to EtOH/POA.

Moreover, melatonin metabolite, N1-acetyl-N1-formyl-5-methoxykynuramine (92), renin-angiotensin system inhibitors (93), and overexpression of pancreatitis-associated protein-1 (94) have been suggested as the potential therapeutic candidates for alcoholic pancreatitis patients by reducing inflammatory and oxidative injury and pancreatic acinar cell death.

In conclusion, DHA inhibits NADPH oxidase activation, increases in ROS levels, and activation of necroptosis-regulating proteins, and prevents mitochondrial dysfunction and thus, suppressing necroptosis of EtOH/POA-treated AR42J cells.

Abbreviations: DCF-DA, dichlorofluorescein diacetate; DHA, docosahexaenoic acid; EtOH, ethanol; FAEEs, fatty acid ethyl esters; MLKL, mixed lineage kinase domain like pseudokinase; MMP, mitochondrial membrane potential; NADPH, nicotinamide adenine dinucleotide phosphate; POA, palmitoleic acid; RIP, receptor interacting protein; ROS, reactive oxygen species.

Authors' contribution: H. Kim conceived of and designed the experiments; J.W. Lim assisted in experimental design; L. Ku, J. Lee, and L. Jin performed the experiments; J.W. Lim and J.T. Seo analyzed the data; L. Ku wrote the paper; H. Kim reviewed and edited the paper. All authors agree with the edited version.

Acknowledgments: Part of this study was presented at 19th Biennial Meeting for the Society for Free Radical Research International (SFRRI) held in Lisbon Congress Center, Lisbon, Portugal, 4 – 7, June, 2018. The abstract of the presentation was published in Free Radical Biology and Medicine 1201(S1), S94-95, 2018 (Abstract Number: P-166).

Conflict of interest: None declared.

REFERENCES

1. Zhu AJ, Shi JS, Sun XJ. Organ failure associated with severe acute pancreatitis. *World J Gastroenterol* 2003; 9: 2570-2573.
2. Shyu JY, Sainani NI, Sahni VA*, et al*. Necrotizing pancreatitis: diagnosis, imaging, and intervention. *Radiographics* 2014; 34: 1218-1239.
3. Raraty MG, Murphy JA, Mcloughlin E, Smith D, Criddle D, Sutton R. Mechanisms of acinar cell injury in acute pancreatitis. *Scand J Surg* 2005; 94: 89-96.
4. Perez S, Pereda J, Sabater L, Sastre J. Redox signaling in acute pancreatitis. *Redox Biol* 2015; 5: 1-14. doi: 10.1016/j.redox.2015.01.014
5. Irving HM, Samokhvalov AV, Rehm J. Alcohol as a risk factor for pancreatitis. A systematic review and meta-analysis. *JOP* 2012; 10: 387-392.
6. Samokhvalov AV, Rehm J, Roerecke M. Alcohol consumption as a risk factor for acute and chronic pancreatitis: a systematic review and a series of meta-analyses. *EBioMedicine* 2015; 2: 1996-2002.
7. Vucevic D, Mladenovic D, Ninkovic M*, et al.* Influence of aging on ethanol-induced oxidative stress in digestive tract of rats. *Hum Exp Toxicol* 2013; 32: 698-705.
8. Norton ID, Apte MV, Lux O, Haber PS, Pirola RC, Wilson JS. Chronic ethanol administration causes oxidative stress in the rat pancreas. *J Lab Clin Med* 1998; 131: 442-446.
9. Rakonczay Z Jr, Boros I, Jarmay K, Hegyi P, Lonovics J, Takacs T. Ethanol administration generates oxidative stress in the pancreas and liver, but fails to induce heat-shock proteins in rats. *J Gastroenterol Hepatol* 2003; 18: 858-867.
10. Ponnappa BC, Hoek JB, Waring AJ, Rubin E. Effect of ethanol on amylase secretion and cellular calcium homeostasis in pancreatic acini from normal and ethanol-fed rats. *Biochem Pharmacol* 1987; 36: 69-79.
11. Del Castillo-Vaquero A, Salido GM, Gonzalez A. Increased calcium influx in the presence of ethanol in mouse pancreatic acinar cells. *Int J Exp Pathol* 2010; 91: 114-124.
12. Chowdhury P, Gupta P. Pathophysiology of alcoholic pancreatitis: an overview. *World J Gastroenterol* 2006; 12: 7421-7427.
13. Fernandez-Sanchez M, del Castillo-Vaquero A, Salido GM, Gonzalez A. Ethanol exerts dual effects on calcium homeostasis in CCK-8-stimulated mouse pancreatic acinar cells. *BMC Cell Biol* 2009; 10: 77. doi: 10.1186/1471-2121-10-77

14. Gonzalez A, Pariente JA, Salido GM. Ethanol impairs calcium homeostasis following CCK-8 stimulation in mouse pancreatic acinar cells. *Alcohol* 2008; 42: 565-573.
15. Gonzalez A, Nunez AM, Granados MP, Pariente JA, Salido GM. Ethanol impairs CCK-8-evoked amylase secretion through Ca2+-mediated ROS generation in mouse pancreatic acinar cells. *Alcohol* 2006; 38: 51-57.
16. Bhopale KK, Falzon M, Ansari GA, Kaphalia BS. Alcohol oxidizing enzymes and ethanol-induced cytotoxicity in rat pancreatic acinar AR42J cells. *In Vitro Cell Dev Biol Anim* 2014: 50: 373-380.
17. Hamamoto T, Yamada S, Hirayama C. Nonoxidative metabolism of ethanol in the pancreas; implication in alcoholic pancreatic damage. *Biochem Pharmacol* 1990; 39: 241-245.
18. Eriksson CJ, Sippel HW. The distribution and metabolism of acetaldehyde in rats during ethanol oxidation. *Biochem Pharmacol* 1977; 26: 241-247.
19. Clemente F, Durand S, Laval J, Thouvenot JP, Ribet A. Ethanol metabolism by rat pancreas. *Gastroenterol Clin Biol* 1977; 1: 39-48.
20. Sarles H, Lebreuil G, Tasso F, *et al*. A comparison of alcoholic pancreatitis. *Gut* 1971; 12: 377-388.
21. Newsome WH, Rattray JB. The enzymatic esterification of pancreatitis and ectopic trypsinogen activation in the rat. *Gastronolenterology* 1995; 109: 239-246.
22. Patton S, McCarthy RD. Conversion of alcohol to ethyl esters of fatty acids by the lactating goat. *Nature* 1966; 209: 616-617.
23. Lange LG, Bergmann SR, Sobel BE. Identification of fatty acid ethyl esters as products of rabbit myocardial ethanol metabolism. *J Biol Chem* 1981; 256: 12968-12973.
24. Doyle KM, Cluette-Brown, JE, Dube DM, Bernhardt TG, Morse CR, Laposata M. Fatty acid ethyl esters in the blood as markers for ethanol intake. *JAMA* 1996; 276: 1152-1156.
25. Laposata M. Fatty acid ethyl esters: short-term and long-term serum markers of ethanol intake. *Clin Chem* 1997; 43: 1527-1534.
26. Laposata EA, Lange LG. Presence of nonoxidative ethanol metabolism in human organs commonly damaged by ethanol abuse. *Science* 1986; 231: 497-499.
27. Werner J, Laposata M, Castillo CF, *et al*. Pancreatic injury in rats induced by fatty acid ethyl ester, a nonoxidative metabolite of alcohol. *Gastroenterology* 1997; 113: 286-294.
28. Wu H, Bhopale KK, Ansari GA, Kaphalia BS. Ethanol-induced cytotoxicity in rat pancreatic acinar cells. Role of fatty acid ethyl esters. *Alcohol Alcoholism* 2008; 43: 1-48.
29. Gerasimenko JV, Gerasimenko OV, Petersen OH. The role of Ca^{2+} in the pathophysiology of pancreatitis. *J Physiol* 2014; 592: 269-280.
30. Criddle DN, Murphy J, Fistetto G, *et al*. Fatty acid ethyl esters cause pancreatic calcium toxicity via inositol trisphosphate receptors and loss of ATP synthesis. *Gastroenterolgy* 2006; 130: 781-793.
31. Huang W, Booth DM, Cane MC, *et al*. Fatty acid ethyl ester synthase inhibition ameliorates ethanol-induced Ca^{2+}-dependent mitochondrial dysfunction and acute pancreatitis. *Gut* 2014; 63: 1313-1324.
32. Hempel N, Trebak M. Crosstalk between calcium and reactive oxygen species signaling in cancer. *Cell Calcium* 2017; 63: 70-96.
33. Kim H. Cerulein pancreatitis: oxidative stress, inflammation, and apoptosis. *Gut Liver* 2008; 2: 74-80.
34. Moyad M. An introduction to dietary/supplemental omega-3 fatty acids for general health prevention: Part II. *Urol Oncol* 2005; 23: 36-48.
35. Lei QC, Wang XY, Xia XF, *et al*. The role of omega-3 fatty acids in acute pancreatitis: a meta-analysis of randomized controlled trials. *Nutrients* 2015; 7: 2261-2273.
36. Holler N, Zarum R, Micheaum O. Fas triggers an alternative, caspase-8-independent cell death pathway using the kinase RIP as effector molecule. *Nat Immunol* 2000; 1: 489-495.
37. Louhimo JM, Steer ML, Perides G. Necroptosis is an important severity determinant and potential therapeutic target in experimental severe pancreatitis. *Cell Mol Gastroenterol Hepatol* 2016; 2: 519-535.
38. Jeong Y, Lim JW, Kim H. Lycopene inhibits reactive oxygen species-mediated NF-κB signaling and induces apoptosis in pancreatic cancer cells. *Nutrients* 2019; 11: 762. doi: 10.3390/nu11040762
39. Kyung S, Lim JW, Kim H. α-lipoic acid inhibits IL-8 expression by activating nrf2 signaling in Helicobacter pylori-infected gastric epithelial cells. *Nutrients* 2019; 11: 2524. doi: 10.3390/nu11102524
40. Lopez E, Figueroa S, Oset-Gasque MJ, Gonzalez MP. Apoptosis and necrosis: two distinct events induced by cadmium in cortical neurons in culture. *Br J Pharmacol* 2003; 138: 901-911.
41. Han H, Lim JW, Kim H. Lycopene inhibits activation of epidermal growth factor receptor and expression of cyclooxygenase-2 in gastric cancer cells. *Nutrients* 2019; 11: 2113. doi: 10.3390/nu11092113
42. Zhao H, Loessberg PA, Sachs G, Muallem S. Regulation of intracellular Ca^{2+} oscillation in AR42J cells. *J Biol Chem* 1990; 265: 20856-20862.
43. Farrar CS, Hocking DC. Assembly of fibronectin fibrils selectively attenuates platelet-derived growth factor-induced intracellular calcium release in fibroblasts. *J Biol Chem* 2018; 293: 18655-8666.
44. Park Y, Lee H, Lim JW, Kim H. Inhibitory effect of β-carotene on Helicobacter pylori-induced TRAF expression and hyper-proliferation in gastric epithelial cells. *Antioxidants* 2019: 8: 637. doi: 10.3390/antiox8120637
45. Kim SH, Lim JW, Kim H. Astaxanthin inhibits mitochondrial dysfunction and interleukin-8 expression in Helicobacter pylori-infected gastric epithelial cells. *Nutrients* 2018; 10: 1320. doi: 10.3390/nu10091320
46. Chan F, Moriwaki K, De Rosa MJ. Detection of necrosis by release of lactate dehydrogenase activity. *Methods Mol Biol* 2013; 979: 65-70.
47. Lugea A, Waldron RT, Mareninova OA, *et al*. Human pancreatic acinar cells: proteomic characterization, physiologic responses, and organellar disorders in ex vivo pancreatitis. *Am J Pathol* 2017; 187: 2726-2743.
48. Shah AP, Mourad MM, Bramhall SR. Acute pancreatitis: current perspectives on diagnosis and management. *J Inflamm Res* 2018; 11: 77-85.
49. Heier C, Xie H, Zimmermann R. Nonoxidative ethanol metabolism in humans - from biomarkers to bioactive lipids. *IUBMB Life* 2016; 68: 916-923.
50. Herreros-Villanueva M, Hijone E, Bafiales JM, Cosme A, Bujanda L. Alcohol consumption on pancreatic diseases. *World J Gastroenterol* 2013; 19: 638-647.
51. Song EA, Lim JW, Kim H. Docosahexaenoic acid inhibits IL-6 expression via PPARγ-mediated expression of catalase in cerulein-stimulated pancreatic acinar cells. *Int J Biochem Cell Biol* 2017; 88: 60-68.
52. Jeong YK, Lee S, Lim JW, Kim H. Docosahexaenoic acid inhibits cerulein-induced acute pancreatitis in rats. *Nutrients* 2017; 9: 744. doi:10.3390/nu9070744
53. Kim SH, Park Y, Lim JW, Kim H. Effect of docosahexaenoic acid on Ca^{2+} signaling pathways in cerulein-treated pancreatic acinar cells, determined by RNA-sequencing

analysis. *Nutrients* 2019; 11: 1445. doi: 10.3390/nu11071445
54. Seo JY, Pandey RP, Lee J, Sohng JK, Namkung W, Park YI. Quercetin 3-O-xyloside ameliorate acute pancreatitis in vitro via the reduction of ER stress ad enhancement of apoptosis. *Phytomedicine* 2019; 55: 40-49.
55. Zhao JY, Wang HQ, Wu L, *et al*. Emodin attenuates cell injury and inflammation in pancreatic AR42J cells. *J Asian Nat Prod Res* 2019; 21: 186-195.
56. Feoktistova M, Leverkus M. Programmed necrosis and necroptosis signalling. *FEBS J* 2015; 282: 19-31.
57. Zhang L, Blackwell K, Workman LM, *et al*. RIP1 cleavage in the kinase domain regulates TRAIL-induced NF-κB activation and lymphoma survival. *Mol Cell Biol* 2015; 35: 3324-3338.
58. Cho Y, Challa S, Moquin D, *et al.* Phosphorylation-driven assembly of the RIP1-RIP3 complex regulates programmed necrosis and virus-induced inflammation. *Cell* 2009; 137: 1112-1123.
59. Cao W-L, Xiang X-H, Chen K, Xu W, Xia SH. Potential role of NADPH oxidase in pathogenesis of pancreatitis. *World J Gastrointest Pathophysiol* 2014; 5: 169-177.
60. Gorlach A, Bertram K, Hudecova S, Krizanova O. Calcium and ROS: a mutual interplay. *Redox Biol* 2015; 6: 260-271.
61. Cui H, Kong Y, Zhang H. Oxidative stress, mitochondrial dysfunction, and aging. *J Signal Transduct* 2012; 2012: 1-13. doi: 10.1155/2012/646354
62. Hernandez-Aguilera A, Rull A, Rodriguez-Gallego E, *et al*. Mitochondrial dysfunction: a basic mechanism in inflammation-related non-communicable diseases and therapeutic opportunities. *Mediators Inflamm* 2013; 2013: 135698. doi: 10.1155/2013/135698
63. Mukherjee R, Criddle DN, Gukvoskaya A, Pandol S, Petersen OH, Sutton R. Mitochondrial injury in pancreatitis. *Cell Calcium* 2008; 44: 14-23.
64. Werner J, Saghir M, Warshaw AL, *et al*. Alcoholic pancreatitis in rats: injury from nonoxidative metabolites of ethanol. *Am J Physiol* 2002; 283: G65-G73.
65. Werner J, Saghir M, Fernandez-del Castillo C, Warshaw AL, Laposata M. Linkage of oxidative and nonoxidative ethanol metabolism in the pancreas and toxicity of nonoxidative ethanol metabolites for pancreatic acinar cells. *Surgery* 2001; 129: 736-744.
66. Criddle DN, Raraty MG, Neoptolemos JP, Tepikin AV, Petersen OH, Sutton R. Ethanol toxicity in pancreatic acinar cells: mediation by nonoxidative fatty acid metabolites. *Proc Natl Acad Sci USA* 2004; 101: 10738-10743.
67. Siech M, Letko G. Influence of ethanol on survival of acinar cells isolated from rat pancreas *Res Exp Med* 1992: 192: 57-63.
68. Nguyen, ST, Nguyen1 HT, Truong KD. Comparative cytotoxic effects of methanol, ethanol and DMSO on human cancer cell lines. *Biomed Res* 2020; 7: 3855-3859.
69. Jamalzadeh L, Ghafoori H, Sariri R, *et al*. Cytotoxic effects of some common organic solvents on MCF-7, RAW-264.7 and human umbilical vein endothelial cells. *Avicenna J Med Biochem* 2016; 4: e33453.
70. Tapani E, Taavitsainen M, Lindros K, Vehmas T, Lehtonen E. Toxicity of ethanol in low concentrations. Experimental evaluation in cell culture. *Acta Radiol* 1996; 37: 923-926.
71. Shimazawa M, Nakajima Y, Mashima Y, Hara H. Docosahexaenoic acid (DHA) has neuroprotective effects against oxidative stress in retinal ganglion cells. *Brain Res* 2009; 1251: 269-275.
72. Liu Q, Wu D, Ni N, *et al*. Omega-3 polyunsaturated fatty acids protect neural progenitor cells against oxidative injury. *Mar Drugs* 2014; 12: 2341-2356.
73. Park KS, Lim JW, Kim H. Inhibitory mechanism of omega-3 fatty acids in pancreatic inflammation and apoptosis. *Ann NY Acad Sci* 2009: 1171: 421-427.
74. Christophe J. Pancreatic tumoral cell line AR42J: an amphicrine model. *Am J Physiol* 1994: 266: G963-G971.
75. Jessow NW, Hay RJ. Characteristics of two rat pancreatic exocrine cell lines derived from transplantable tumors. [Abstract]. *In vitro* 1980; 16: 212.
76. Szmola R, Sahin-Toth M. Pancreatitis-associated chymotrypsinogen C (CTRC) mutant elicits endoplasmic reticulum stress in pancreatic acinar cells. *Gut* 2010; 59: 365-372.
77. Gonzalez A, Santofimia-Castano P, Salido G. Culture of pancreatic AR42J cell for use as a model for acinar cell function. Pancreapedia: Exocrine Pancreas Knowledge Base 2011;Version 1.0:2011. doi: 10.3998/panc.2011.26
78. Logsdon CD, Moessner A, Williams JA, Goldfine ID. Glucocorticoids increase amylase mRNA levels, secretory organelles, and secretion in pancreatic acinar AR42J cells. *J Cell Biol* 1985; 100: 1200-1208.
79. Logsdon CD. Glucocorticoids increase cholecystokinin receptors and amylase secretion in pancreatic acinar AR42J cells. *J Biol Chem* 1986; 261: 2096-2101.
80. Rajasekaran AK, Morimoto T, Hanzel DK, Rodriguez-Boulan E, Kreibich G. Structural reorganization of the rough endoplasmic reticulum without size expansion accounts for dexamethasone-induced secretory activity in AR42J cells. *J Cell Sci* 1993; 105: 333-345.
81. Singh L, Bakshi DK, Vasishta RK, Arora SK, Majumdar S, Wig JD. Primary culture of pancreatic (human) acinar cells. *Dig Dis Sci* 2008; 53: 2569-2575.
82. Liu J, Akanuma N, Liu C, *et al*. TGF-β1 promotes acinar to ductal metaplasia of human pancreatic acinar cells. *Sci Rep* 2016; 6: 30904. doi: 10.1038/srep30904
83. Ji B, Bi Y, Simeone D, Mortensen RM, Logsdon CD. Human pancreatic acinar cells lack functional responses to cholecystokinin and gastrin. *Gastroenterology* 2001; 121: 1380-1390.
84. Dong W, Li Z, Chen Y, *et al*. NADPH oxidase inhibitor, diphenyleneiodonium prevents necroptosis in HK-2 cells. *Biomed Rep* 2017; 7: 226-230.
85. Goossens V, De Vos K, Vercammen D, *et al*. Redox regulation of TNF signaling. *BioFactors* 1999; 10: 145-156.
86. Schulze-Osthoff K, Bakker AC, Vanhaesebroeck B, Beyaert R, Jacob WA, Fiers W. Cytotoxic activity of tumor necrosis factor is mediated by early damage of mitochondrial functions. Evidence for the involvement of mitochondrial radical generation. *J Biol Chem* 1992; 267: 5317-5323.
87. Schulze-Osthoff K., Beyaert R, Vandevoorde V, Haegeman G, Fiers W. Depletion of the mitochondrial electron transport abrogates the cytotoxic and gene-inductive effects of TNF. *EMBO J* 1993; 12: 3095-3104.
88. Schenk B, Fulda S. Reactive oxygen species regulate Smac mimetic/TNFα-induced necroptotic signaling and cell death. *Oncogene* 2015; 34: 5796-5806.
89. Zhang Y, Su SS, Zhao S, *et al.* RIP1 autophosphorylation is promoted by mitochondrial ROS and is essential for RIP3 recruitment into necrosome. *Nat Commun* 2017; 8: 14329. doi: 10.1038/ncomms14329
90. Yu X, Deng Q, Li W, *et al*. Neoalbaconol induces cell death through necroptosis by regulating RIPK-dependent autocrine TNF-α and ROS production. *Oncotarget* 2015; 6: 1995-2008.
91. Shindo R, Kakehashi H, Okumura K, Kumagai Y, Nakano H. Critical contribution of oxidative stress to TNF-α-induced necroptosis downstream of RIPK1 activation. *Biochem Biophys Res Commun* 2013; 436: 212-216.

92. Jaworek J, Szlarczyk J, Bonior J, *et al*. Melatonin metabolite, N1-acetyl-N1-formyl-5-methoxykynuramine (AFMK), attenuates acute pancreatitis in the rat in vivo and in vitro studies. *J Physiol Pharmacol* 2016; 67: 411-421.
93. Madro A, Kurzepa J, Celinski K, *et al*. Effects of renin-angiotensin system inhibitors on fibrosis in patients with alcoholic chronic pancreatitis. *J Physiol Pharmacol* 2016; 67: 103-110.
94. Yu JH, Lim JW, Kim H. Pancreatitis-associated protein-1 suppresses apoptosis in cerulein-stimulated pancreatic acinar cells in response to nuclear factor-κB activation. *J Physiol Pharmacol* 2019; 70: 849-857.

Received: May 18, 2020
Accepted: June 30, 2020

Author's address: Prof. Hyeyoung Kim, Department of Food and Nutrition, College of Human Ecology, Yonsei University, Seoul 03722, Republic of Korea.
E-mail: kim626@yonsei.ac.kr